

Structure of the Si(111)-(5 × 2)-Au Surface

Tadashi Abukawa and Yoshiki Nishigaya

Institute of Multidisciplinary Research for Advanced Materials, Tohoku University, Sendai 980-8577, Japan
(Received 31 August 2012; published 15 January 2013)

The structure of the Si(111)-(5 × 2)-Au surface, one of the long-standing problems in surface science, has been solved by means of Weissenberg reflection high-energy electron diffraction. The arrangement of the Au atoms and their positions with respect to the substrate were determined from a three-dimensional Patterson function with a lateral resolution of 0.3 Å based on a large amount of diffraction data. The new structural model consists of six Au atoms in a 5 × 2 unit, which agrees with the recently confirmed Au coverage of 0.6 ML [I. Barke *et al.*, Phys. Rev. B **79**, 155301 (2009)]. The model has a distinct ×2 periodicity, and includes a Au dimer. The model is also compatible with previously obtained STM images.

DOI: 10.1103/PhysRevLett.110.036102

PACS numbers: 68.65.-k, 61.05.jh, 68.35.bg

Introduction.—Since its surface was first reported in 1969 [1], Si(111)-(5 × 2)-Au has been widely studied because of its strong one dimensionality. In particular, one-dimensional (1D) chain structures were an expected prototype of a one-dimensional metal on a two-dimensional surface [2]. In addition to 5 × 2-Au, a variety of Au chain structures were observed on vicinal substrates of Si(111), and their 1D metallic states were extensively investigated by photoemission studies [3–5]. In order to understand the one-dimensional metallicity of the system, structural information is essential.

Several structural models were proposed for the 5 × 2-Au surface by several techniques [6–16]. However, no consensus has yet been achieved on the structure model. The Au coverage was believed to be 0.4 ML based on a macroscopic determination in early studies. For example, Marks and Plass proposed a structural mode by transmission electron diffraction and high resolution electron microscopy [11], and first-principles studies proposed other 0.4 ML models [13,14]. Although most of the models commonly included two Au chains in a 5 × 2 unit cell, their detailed arrangements were different. Recently, however, Barke *et al.* precisely determined the Au coverage of 5 × 2-Au domains by STM, and surprisingly revised the Au coverage to be 0.6 ML [17]. Then, a new structural model with 0.6 ML of Au, which included triple Au chains, was proposed in the first-principles study [15].

Unfortunately, no crystallographic technique has been applied to this surface since the transmission electron diffraction study [11]. In this work, we applied Weissenberg reflection high-energy electron diffraction (W-RHEED) [18] to the Si(111)-(5 × 2)-Au surface to investigate the surface structure.

There are at least four inherent difficulties in the structural analysis of the 5 × 2-Au surface: (1) the large unit cell with onefold symmetry, (2) triple orientations on the threefold substrate, (3) incoherent arrangements of the 5 × 2 lattice, and (4) partial occupation of Si adatoms.

Difficulty (1) can be resolved by collecting sufficient data, i.e., a number of diffraction patterns. We can overcome (2) by using a single-domain surface, which can be produced on a slightly vicinal Si(111) substrate [19,20]. Problem (3) may be the most serious obstacle with regard to structural analysis. Only streaky diffraction patterns can be observed for the 5 × 2-Au surface, instead of half-order spots. These streaks were interpreted as incoherent arrangements of 5 × 2 units, as observed by STM [10,21]. As schematically shown in Fig. 1, so-called *Y* units were observed in rectangular 5 × 2 units, and formed rows along the $[1\bar{1}0]$ direction with ×2 periodicity. There are two possible arrangements of neighboring rows that can fulfill the 5 × 2 periodicity. One arrangement forms a 5 × 2A lattice, and the other forms a 5 × 2B lattice, as shown in Fig. 1. An incoherent arrangement of 5 × 2A and 5 × 2B lattices causes streaks instead of half-order spots.

Therefore, only spots corresponding to 5 × 1 periodicity are available for the structural analysis of 5 × 2-Au, in which the 5 × 2 structure is folded into a 5 × 1 unit cell.

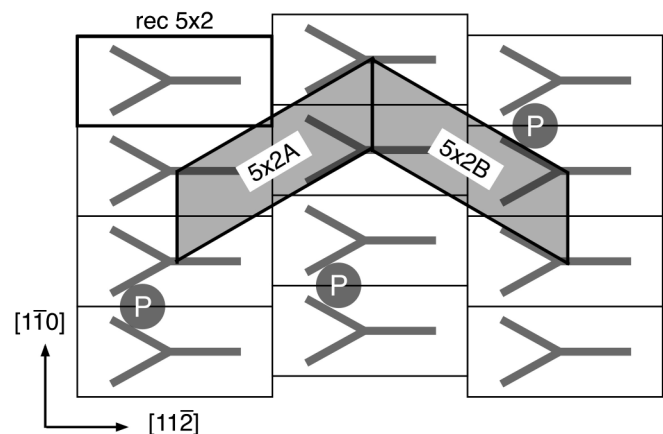


FIG. 1. Arrangement of unit cells on the 5 × 2-Au surface. Characteristic features of STM images, i.e., *Y* units and Si adatoms *P*, are overlaid based on the literature [10,21]. Different arrangements of the rectangular units cause two types of 5 × 2 units.

In order to recover the 5×2 structure from this folded structure, a high spatial resolution is required in the structural analysis.

Another important type of information obtained from the STM images is item (4) above, the partial occupation of Si adatoms [10,21]. The adatoms showed up in specific sites, indicated in Fig. 1 as P , with an occupation ratio of $\sim 25\%$. The influence of the adatoms must be considered in the structural analysis.

In order to overcome these difficulties, we obtained a large amount of diffraction data for the single-domain Si (111)-(5×2)-Au surface by W-RHEED. Although only 5×1 spots were used in the present study, the 5×2 -Au structure has been successfully recovered from the large amount of data obtained.

Experiment.—The following experiments were performed in a UHV chamber equipped with RHEED optics, a retarding field energy filter, and a hemispherical electron analyzer for Auger electron spectroscopy [22,23]. An electron beam with a kinetic energy of 10 keV was used for the RHEED measurements and Auger electron spectroscopy. A Si(111) wafer with an intentional miscut of 1° was used in order to obtain a single-domain 5×2 -Au surface. The wafer was cut into $20 \times 4.0 \times 0.4$ mm³ and carefully out-gassed in UHV by resistive heating below 700°C . Then, the wafer was cleaned by annealing at 1000°C for several minutes and flashing at 1250°C for 5 sec. Gold was deposited on a clean 7×7 surface from a hot tungsten filament wetted by gold. The best single-domain 5×2 -Au was obtained when Au with a $\sim 10\%$ excess for the optimum 5×2 -Au phase was deposited on the RT substrate, and then annealed at 850°C for a few minutes. The single-domain 5×2 -Au surface was cooled to -120°C by LN₂ flow during the W-RHEED measurements.

In order to cover the entire 2π azimuth, we measured ~ 600 RHEED patterns as a function of the sample-azimuth rotation with an interval of 0.2° from a $[11\bar{2}]$ incident azimuth toward a $[1\bar{1}0]$ incident [24]. Two opposite quadrants in k space were covered by the scan. The two quadrants were extended into the 2π range using the mirror symmetry of the surface. We measured five W-RHEED scans with different incident angles of 2.0° , 2.5° , 3.0° , 4.0° , and 5.0° . A three-dimensional (3D) k map, which is the intensity as a function of the scattering vector \mathbf{s} , was obtained from each scan. Only elastically scattered electrons were selected by the energy filter. Then, the five k maps were summed up into a total k map, and a 3D Patterson map, $P(\mathbf{r})$, was calculated as a modulus of the Fourier transform of the total k map.

Results and discussion.—A horizontal section of the k map at an incident angle of 2.5° [24] is shown in Fig. 2. (It should be noted that the spots are elongated along the radial direction from the origin in the k map because of the finite spot size on the screen.) The positions of the 5×1 spots and $\times 2$ streaks are schematically overlaid on the right upper corner of the image. As seen in the k map,

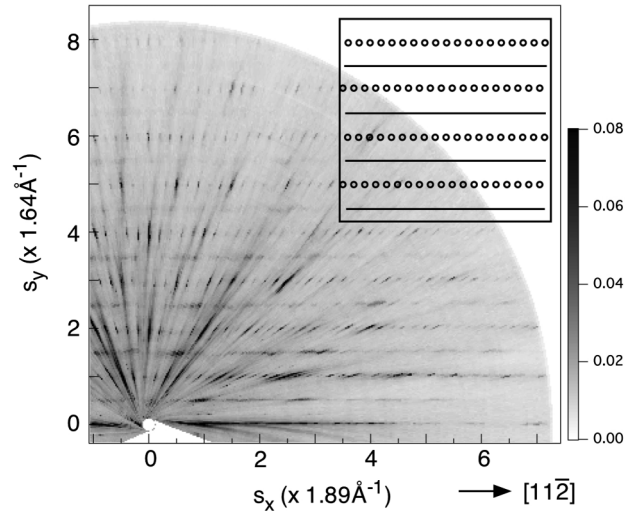


FIG. 2. Horizontal section at $s_z = 8.5 \text{ \AA}^{-1}$ of the k map with an incident angle of 2.5° . Only one quadrant is shown.

we obtained a nearly perfect single domain of 5×2 -Au. We used all of the spot intensities to make the 3D k map, and the size of the 3D map was $\sim 25 \text{ \AA}^{-1}$ and $\sim 15 \text{ \AA}^{-1}$ in the horizontal and vertical directions, respectively [18]. Therefore, the present k map has real-space resolutions of $\sim 0.3 \text{ \AA}$ in the lateral direction and $\sim 0.5 \text{ \AA}$ in the vertical direction. This high spatial resolution was the key to solving the present structure.

Two important sections of $P(\mathbf{r})$, at $z = 0.0 \text{ \AA}$ and -3.1 \AA , are shown in Figs. 3(a) and 3(b), respectively. The intensity was normalized by the strongest intensity at the origin. The sections were extended repeatedly into the rectangular 5×2 unit (see Fig. 1). In addition to the inherent inversion symmetry, $P(\mathbf{r})$ has a mirror symmetry about the xz plane. Within the Born approximation, $P(\mathbf{r})$ is a self-convolution of the atomic potentials by the structure, so that atomic pairs in the structure will be mapped as spots in $P(\mathbf{r})$. The atomic potentials for Au and Si were calculated from the atomic wave function [25]. The magnitude of the calculated atomic potential for Si was about 30% that of Au when the thermal vibration at -120°C was considered. Thus, the relative intensity of Au-Au, Au-Si, and Si-Si pairs in $P(\mathbf{r})$ were estimated to be 1, 0.3, and 0.09, respectively. The present $P(\mathbf{r})$ is sensitive to the structure of the heavy Au atoms.

The section at $z = 0.0 \text{ \AA}$ in Fig. 3(a) corresponds to the pair-distribution map of the atoms in the same plane, where most of the Au-Au pairs should be located. Strong spots were arranged on a 1×1 lattice in this section. These strong spots mainly originated from the 1×1 arrangement of the substrate Si. In addition to these strong 1×1 spots, there were notable structures surrounding the 1×1 spots at $x = \pm 3.3 \text{ \AA}$. These structures were $\sim 0.5 \text{ \AA}$ away from the 1×1 spots in the y direction. As indicated by the arrows in Fig. 3(a), the distance between the neighboring

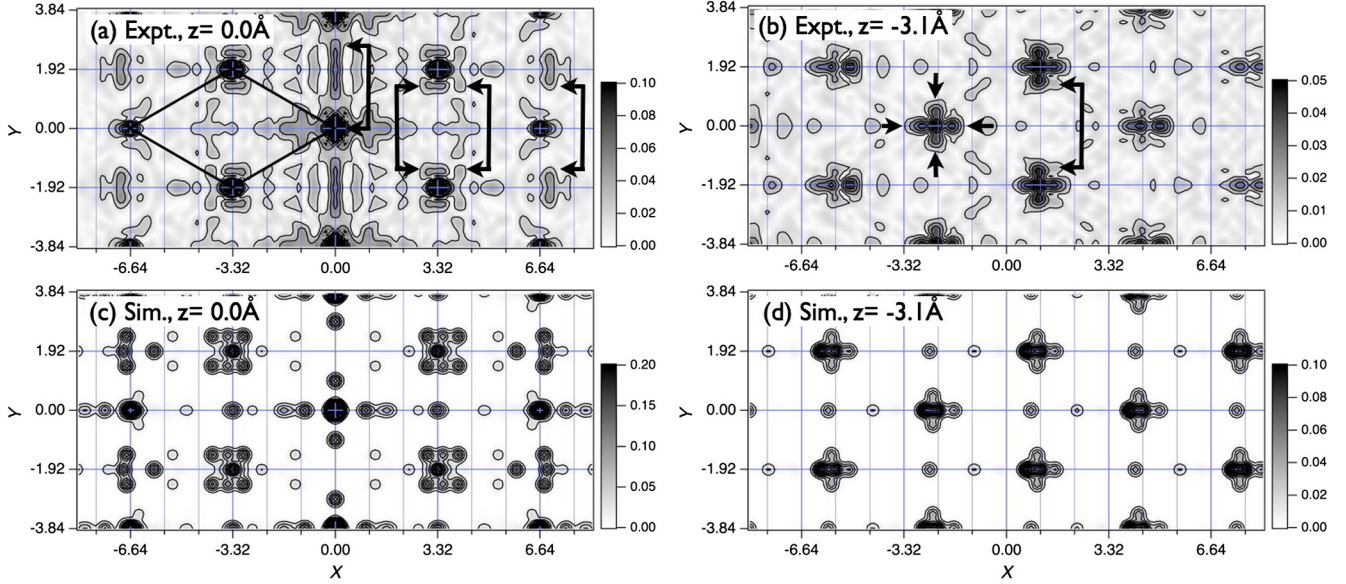


FIG. 3 (color online). Sections of Patterson function $P(\mathbf{r})$: (a) and (b) are sections of the experimental pattern at $z = 0.0 \text{ \AA}$ and -3.1 \AA , respectively. (c) and (d) are simulations using the present model (see text). A 1×1 unit is shown in (a).

structures was close to the metal bond length of Au (2.85 \AA). We found several structures corresponding to the Au-Au bond length in the y direction, as shown in Fig. 3(a). It is probable that Au-Au bonds oriented along the y direction exist on the 5×2 -Au surface.

Below $z = -1.0 \text{ \AA}$, the most intense structures were observed at $z = -3.1 \text{ \AA}$ as shown in Fig. 3(b). These should correspond to pairing between Au atoms and the underlying Si substrate. In Fig. 3(b), “four-petal flower” shapes appear, and these are arranged on a 1×1 lattice. As indicated by the short arrows in Fig. 3(b), the four petals consist of at least four spots surrounding the bulk central spot. If Au atoms simply replaced the top Si atoms of the ideal Si(111) surface, the four spots would overlap with the bulk spot. As shown in Fig. 3(b) by the connecting arrow, the existence of the Au dimer is also suggested.

The present $P(\mathbf{r})$ strongly suggests the existence of the Au dimer. We took the correlation between the dimer and the $P(\mathbf{r})$ by using the minimum function method to solve the Patterson function [18]. The minimum function $M(\mathbf{r})$ by the dimer unit is simply the minimum value at \mathbf{r} of the two shifted $P(\mathbf{r})$ as follows:

$$M(\mathbf{r}) = \text{Min} \left\{ P\left(\mathbf{r} - \frac{\mathbf{r}_1}{2}\right), P\left(\mathbf{r} + \frac{\mathbf{r}_1}{2}\right) \right\}, \quad (1)$$

where $\mathbf{r}_1 = (0, 2.84, 0)$. We set $P(\mathbf{r})$ to zero at $0.2 < |\mathbf{r}| < 1.5 \text{ \AA}$ to suppress the artifacts in $M(\mathbf{r})$. The atomic arrangement viewed from the Au dimer would be depicted in the $M(\mathbf{r})$.

Sections of $M(\mathbf{r})$ at $z = 0.0 \text{ \AA}$ and -3.1 \AA are shown in Figs. 4(a) and 4(b), respectively. The D_1 and D_2 spots are the Au dimer. The intense structures around $(0, \pm 3.84)$ are too close to D_1 or D_2 and are probably artifacts from the

origin peak that extended to the 5×2 unit. Besides these, there are additional intense spots labeled A , B , C , and E in Fig. 4(a). Because $M(\mathbf{r})$ at $z = 0.0 \text{ \AA}$ has mirror symmetry about both x and y axes and 5×1 symmetry except around D_1 and D_2 , there are four equivalent spots for each of A , B , C , and E in the 5×2 unit. One out of four spots for each of A , B , C , and E will be the position of the Au atom, so the number of Au atoms in the 5×2 unit is consistent with 0.6 ML of coverage [17]. If one correctly selects the Au sites for each of A , B , C , and E , then the arrangement of the Au will be determined.

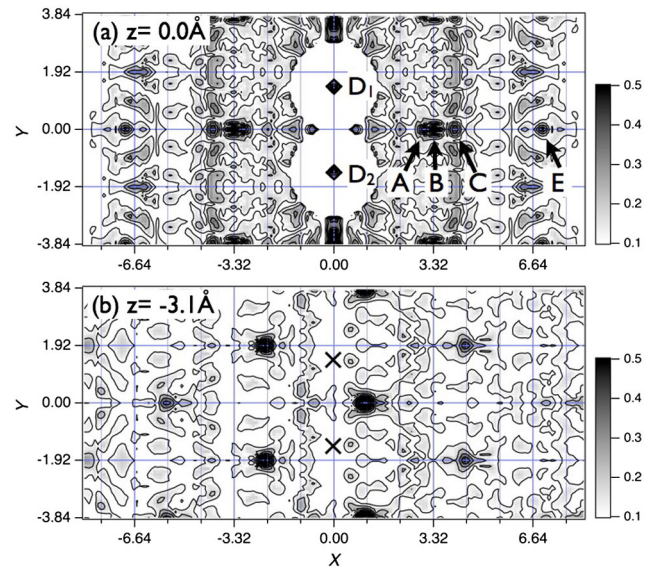


FIG. 4 (color online). Sections of the minimum function $M(\mathbf{r})$ of the Au dimer: (a) at $z = 0.0 \text{ \AA}$ and (b) at $z = -3.1 \text{ \AA}$.

The section of $M(\mathbf{r})$ at $z = -3.1 \text{ \AA}$ in Fig. 4(b) is surprisingly simple. Strong spots are arranged on a 1×1 lattice in the figure. These should be the unreconstructed substrate atoms viewed from the Au dimer. This simple interpretation strongly supports the existence of the Au dimer. Now, we have the registry of the Au dimer atoms to the substrate, as indicated by the X marks in Fig. 4(b).

Based on the structural information obtained above, we further analyzed the surface structure by trial and error comparison between the experimental Patterson function and the simulated one for the model structures. For the simulation of the Patterson function, we followed the kinematical diffraction process. First, we approximated the atomic potentials of Au and Si as three-dimensional Gaussians. This was a reasonable approximation, considering the thermal vibration and the limited experimental window. The Gaussian potentials were placed at the atomic positions of the model structures. We used a rectangular 10×2 lattice, which included two shifted 5×2 units for computational reasons, although the irreducible unit was the rectangular 5×2 unit. Then, the diffraction intensity was obtained from the Fourier transform of the arranged potential. Finally, a simulated $P(\mathbf{r})$ was calculated from the Fourier transformation of the simulated intensity, using only the 5×1 spots.

More than a hundred Patterson functions were calculated based on the structure models. Only the structures within the framework suggested by the minimum function gave plausible Patterson functions to fit the experimental one. Finally, the most plausible model, which was also consistent with the STM images, was obtained, as shown by a ball and stick atomic model in Fig. 5. Six gold atoms were located within the unit in accordance with the framework suggested by the minimum function, and these are

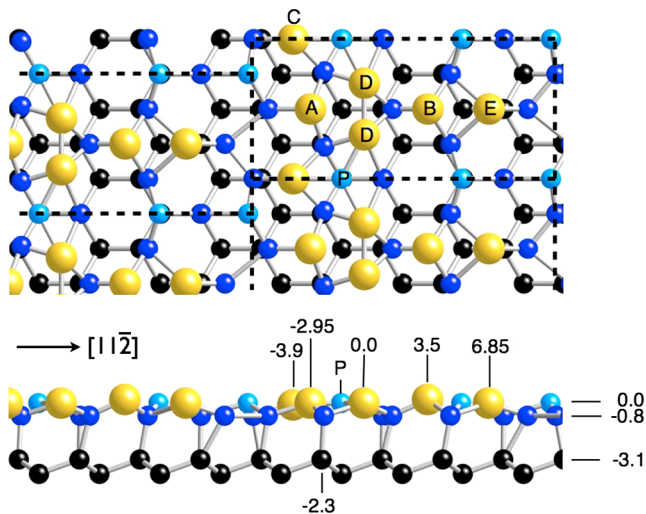


FIG. 5 (color online). Ball-and-stick model of the Si(111)- 5×2 -Au surface proposed in the present study. Large and small spheres represent Au and Si atoms, respectively. x and z coordinates relative to the Au dimer are indicated.

labeled using the same notation as was used in Fig. 4(a). The six gold atoms form a tiny “Eiffel tower” laying sideways on the Si surface. The Au arrangement and the Si adatom position P are compatible with the Y -shaped structure and the Si adatoms of STM images [10]. For further discussion regarding the STM images, theoretical studies of the present model are highly desired.

Sections at $z = 0.0 \text{ \AA}$ and -3.1 \AA of the simulated $P(\mathbf{r})$ based on the present model are shown in Figs. 3(c) and 3(d), respectively. The simulation reproduced most of the distinct features of the experimental sections. There was very good agreement at the sections of $z = -3.1 \text{ \AA}$. However, some discrepancies remain. For example, there is a strong spot at $(5.7, 1.92)$ in Fig. 3(c) that is not present in the experimental section. This spot corresponds to Au-Au atomic pair crossing between neighboring units. Such atomic pair positions would be influenced by the incoherent arrangement of the units.

Other faint structures, which were not reproduced by the simulation, were related to the surface Si atoms. We tried to optimize these Si atoms in the present 5×2 -Au model. However, it was impossible to determine a number of Si positions using the present $P(\mathbf{r})$ because of the uncertainty induced by the incoherent arrangement and the adatoms. Therefore, we placed 1 ML of surface Si atoms just above the substrate Si atoms, then relaxed them to have reasonable bond lengths with Au. Afterwards, we placed Si adatoms to terminate the dangling bonds remaining in the structure.

Although we could not optimize the surface Si atoms, the present model reproduced the experimental $P(\mathbf{r})$ fairly well, as shown in Fig. 3. The present model and the structural framework will be a good starting point for further detailed experimental and theoretical studies. Here, we comment on the Si honeycomb chain, which was expected for the 5×2 -Au surface according to previous theoretical work [13–15]. The present results are negative to the Si honeycomb chain because there is no space for it between the Au atoms.

Conclusion.—The structure of Si(111)- (5×2) -Au was solved by W-RHEED. The 3D Patterson function with a lateral resolution of 0.3 \AA was obtained, and was solved by means of the minimum function method. The arrangement of the Au atoms and their positions with respect to the substrate were determined. The new model consists of six gold atoms in a 5×2 unit, which agrees with the recently confirmed Au coverage of 0.6 ML [17]. The model has distinct $\times 2$ periodicity, and includes Au dimers. The model is compatible with the Y -shaped structure and Si adatoms observed in STM images. The one-dimensional metallicity of the surface should be reconsidered in light of the present model.

This work was supported in part by Grants-in-Aid for Scientific Research (B) Grant No. 17360016 and Scientific Research (A) Grant No. 20244042 from JSPS.

- [1] H. E. Bishop and J. C. Rivière, *J. Phys. D* **2**, 1635 (1969).
- [2] I. Collins, J. Moran, P. Andrews, R. Cosso, J. O'Mahony, J. McGilp, and G. Margaritondo, *Surf. Sci.* **325**, 45 (1995).
- [3] J. N. Crain, A. Kirakosian, K. N. Altmann, C. Bromberger, S. C. Erwin, J. L. McChesney, J.-L. Lin, and F. J. Himpsel, *Phys. Rev. Lett.* **90**, 176805 (2003).
- [4] J. N. Crain, J. L. McChesney, F. Zheng, M. C. Gallagher, P. C. Snijders, M. Bissen, C. Gundelach, S. C. Erwin, and F. J. Himpsel, *Phys. Rev. B* **69**, 125401 (2004).
- [5] I. Matsuda, M. Hengsberger, F. Baumberger, T. Greber, H. W. Yeom, and J. Osterwalder, *Phys. Rev. B* **68**, 195319 (2003).
- [6] G. Le Lay, *J. Cryst. Growth* **54**, 551 (1981).
- [7] L. E. Berman, B. W. Batterman, and J. M. Blakely, *Phys. Rev. B* **38**, 5397 (1988).
- [8] E. Bauer, *Surf. Sci.* **250**, L379 (1991).
- [9] C. Schamper, W. Moritz, H. Schulz, R. Feidenhansl, M. Nielsen, F. Grey, and R. L. Johnson, *Phys. Rev. B* **43**, 12130 (1991).
- [10] J. D. O'Mahony, C. H. Patterson, J. F. McGilp, F. M. Leibsle, P. Weightman, and C. F. J. Flipse, *Surf. Sci.* **277**, L57 (1992).
- [11] L. D. Marks and R. Plass, *Phys. Rev. Lett.* **75**, 2172 (1995).
- [12] T. Hasegawa, S. Hosaka, and S. Hosoki, *Surf. Sci.* **357–358**, 858 (1996).
- [13] S. C. Erwin, *Phys. Rev. Lett.* **91**, 206101 (2003).
- [14] S. Riikonen and D. Sánchez-Portal, *Phys. Rev. B* **71**, 235423 (2005).
- [15] S. C. Erwin, I. Barke, and F. J. Himpsel, *Phys. Rev. B* **80**, 155409 (2009).
- [16] H. S. Yoon, J. E. Lee, S. J. Park, I.-W. Lyo, and M.-H. Kang, *Phys. Rev. B* **72**, 155443 (2005).
- [17] I. Barke, F. Zheng, S. Bockenhauer, K. Sell, V. Oeynhaus, K. Meiwes-Broer, S. Erwin, and F. Himpsel, *Phys. Rev. B* **79**, 155301 (2009).
- [18] T. Abukawa, T. Yamazaki, K. Yajima, and K. Yoshimura, *Phys. Rev. Lett.* **97**, 245502 (2006).
- [19] J. R. Power, P. Weightman, and J. D. O'Mahony, *Phys. Rev. B* **56**, 3587 (1997).
- [20] D. Tsukanov, S. Ryjkov, O. Utas, and V. Lifshits, *Appl. Surf. Sci.* **234**, 297 (2004).
- [21] A. Kirakosian, J. Crain, J.-L. Lin, J. McChesney, D. Petrovykh, F. Himpsel, and R. Bennewitz, *Surf. Sci.* **532–535**, 928 (2003).
- [22] T. Abukawa, D. Fujisaki, N. Takahashi, and S. Sato, *e-J. Surf. Sci. Nanotechnol.* **7**, 866 (2009).
- [23] T. Abukawa, S. Sato, and Y. Matsuoka, *Surf. Sci.* **604**, 1614 (2010).
- [24] See Supplemental Material at <http://link.aps.org/supplemental/10.1103/PhysRevLett.110.036102> for movies of the RHEED patterns during the sample-azimuth rotation and the 3D reciprocal map obtained by a single scan of the present W-RHEED. The latter one was created by the software OSIRIX.
- [25] E. Clementi and C. Roetti, *At. Data Nucl. Data Tables* **14**, 177 (1974).